BRL R 1445

BRL

AD

REPORT NO. 1445

EXPERIMENTAL AND NUMERICAL NONEQUILIBRIUM FLOW STUDIES

by

J. H. Spurk

May 1969

U.S. ARMY ABERDEEN RESEARCH AND DEVELOPMENT CENTER
BALLISTIC RESEARCH LABORATORIES
ABERDEEN PROVING GROUND, MARYLAND

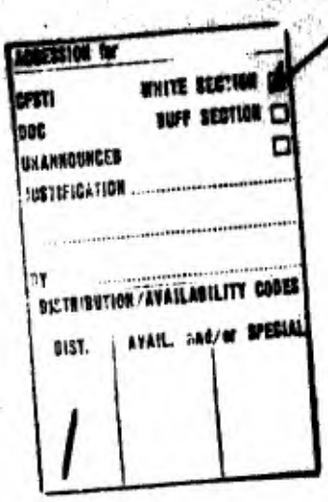

Destroy this report when it is no longer needed.
Do not return it to the originator.

The findings in this report are not to be construed as an official Department of the Army position, unless so designated by other authorized documents.

The use of trade names or manufacturers' names in this report does not constitute indorsement of any commercial product.

BALLISTIC RESEARCH LABORATORIES

REPORT NO. 1445

MAY 1969

EXPERIMENTAL AND NUMERICAL NONEQUILIBRIUM FLOW STUDIES

J. H. Spurk

Exterior Ballistics Laboratory

RDT&E Project No. 1T061102A33D

ABERDEEN PROVING GROUND, MARYLAND

B A L L I S T I C R E S E A R C H L A B O R A T O R I E S

REPORT NO. 1445

JHSpurk/beh
Aberdeen Proving Ground, Md.
May 1969

EXPERIMENTAL AND NUMERICAL NONEQUILIBRIUM FLOW STUDIES

ABSTRACT

Experimental and numerical studies of the nonequilibrium shock layer around cones in hypersonic pure oxygen flows are reported. Experimental conditions are such that rotational, vibrational and dissociation relaxation occur simultaneously. Attention is given to the effect of coupled relaxation on the flow properties in the shock layer. The phenomenological models of Hammerling, et al, and Treanor and Marrone predict the flow field qualitatively correct. However, quantitative differences in shock geometry and density distribution are appreciable. Better quantitative agreement with experiment is reached if in these models a temperature dependent efficiency of O_2 and O in the relaxation processes is assumed.

TABLE OF CONTENTS

LIST OF ILLUSTRATIONS

BLANK PAGE

I. INTRODUCTION

For certain flight conditions, the flow field around the body is to a large extent determined by the rate with which various relaxation processes occur. In the past much effort has been devoted to the numerical prediction of these flow fields. The analysis assumes a gas model by specifying the relaxation equations and the equations of state. The most commonly used gas models assume only one relaxation process with equilibrium or frozen conditions existing for the remaining internal modes. This appreciable simplification is possible if the relaxation times characterizing the various relaxation processes are vastly different, with the relaxation time of the dominant process in the order of the flow time L/U_∞. For example, the gas model which assumes translational, rotational and vibrational equilibrium, frozen ionization, and which considers as the only relaxation processes dissociation and recombination, has been widely used[1,2,3] even outside its range of applicability to predict the flow fields around bodies in hypersonic flight. Such a model is only valid in a regime where the inequalities $\tau_{tr} < \tau_{rot} < \tau_{vib} << \tau_{diss} << \tau_{ion}$ hold and where $\tau_{diss} \sim 0(L/U_\infty)$. Experimental studies[4] of the flow field around cones have confirmed the adequacy of this model for these conditions. For a temperature above 8,000°K in the shock layer the above inequalities cease to be valid for the oxygen component, and simultaneous vibrational and dissociation relaxation occur. The two processes interact with each other, so that the overall relaxation is largely affected.

Phenomenological rate equations[5] accounting for the vibration dissociation coupling have been used to compute the reaction profiles behind strong normal shocks in air. Comparison with experimental data[6] in terms of half-decomposition distance of the oxygen component shows the experimental distance to be substantially larger than the theoretical value. For the case of interest here, i.e. the hypersonic flow around a body, departure of experiments from prediction should be expected all the more, because the relaxation process is additionally affected by the gas dynamic process.

It is the purpose of this paper to report experimental data on the shock layer flow for free stream conditions where considerable coupling between rotation, vibration, and dissociation exists, their respective relaxation times being of the same order of magnitude when extrapolated to the condition of the experiments. The experimental results are compared with numerical prediction of the flow field. Since at present there is no theory to describe this coupled relaxation process, the gas models on which the computations are based are simplified in various respects, mainly one or several of the pertinent relaxation times are assumed zero or infinite.

The test gas was pure oxygen rather than air to avoid additional complexities associated with a mixture of diatomic gases. On the other hand, the significant effects of relaxation under non-isothermal conditions are preserved. Oxygen is a good choice for the present purpose because its reaction kinetics have been most extensively studied.

II. EXPERIMENTS

The hypersonic high energy flow of pure oxygen is generated in an expansion tube[7]. The expansion tube for one of the experiments is operated in such a manner as to avoid any free stream dissociation, i.e. the compressibility $Z_\infty = 1$.

In this case, subsequently referred to as case 1 the free stream condition is determined by the measurement of free stream density and free stream pressure. The free stream vibrational energy may be somewhat higher than indicated by the translational temperature $T_\infty = p_\infty (\rho_\infty R)^{-1}$. For the other experiment (case 2) the expansion tube is operated in the reflected mode; this may result in a free stream nonequilibrium condition with $Z_\infty \sim 1.1$ where neither the state of dissociation nor the vibrational energy is in equilibrium with the translational temperature. The free stream density measurement is made by streak interferometry. The accuracy of this measurement is affected by two errors; the random error in measuring the fringe shift, which is about 10%, and a systematic error resulting from the fact that the light beam traverses the boundary layer

on the observation windows of the expansion tube[8]. The latter error can be corrected in an approximate way. The combined error is not larger than 20% and measured free stream density is adjusted within this bound as described in section VI. Impurity concentrations in the shock layer have been measured for conditions similar to the condition of these experiments. The concentration of the main contaminants Fe, Cr, CN was found to be less that 400ppm[9]. The test gas prior to admission into the facility has been checked for nitrogen contamination which was found to be less than 10ppm. For the actual test, the gas is at relatively high pressure ($\sim$1/2 Atm) so that contamination by residual air in the tube (50 μ Hg) is small.

These impurity concentrations are too small to affect the relaxation process especially at the high shock layer temperatures of these experiments.

The main experimental tool is a Mach-Zehnder optical interferometer which is used to observe, without interference, the stationary flow around the model and the free stream flow. The frame interferograms of the two flow fields are shown in Figures 1 and 2. The model diameter is 2 inches in both cases; the cone angles 45° and 35° respectively.

From these interferograms one can determine the shock position and the fringe shift, i.e. the difference of ordinates of the undisturbed and the disturbed fringe in an x,r coordinate system attached to the apex of the cone. x is measured along the axis of the cone and r normal to x. It is convenient to measure the fringe shift along traces x = constant and to present the data as a function of the distance r from the axis along x = constant. The actual measurement of the fringe shift is done automatically on a fringe reader; the shock position is measured manually on the same instrument. The fringe reader is essentially a microscope in conjunction with a light sensitive cell. The position of the fringes is found from the variation in back light intensity as the interferogram is scanned.

The experimental fringe shift and shock shape are the principal data which are used in the comparison with numerical predictions.

III. NUMERICAL COMPUTATIONS

For the free stream conditions of the experiments, the flow around the conical bodies is purely supersonic and the method of characteristics can be used to integrate numerically the equations of motion together with the rate equations. Once a gas model is specified the integration is rather routine; however, care must be taken to insure reliability of the numerical results. The correctness of the characteristic solution can be judged by comparing its behavior to the simpler conical flow solution of frozen and equilibrium flows. The stream function on the body is computed for each advance in right-running characteristic. The value of the stream function at the body is kept to 1% of the value at the shock for the same characteristic.

From the numerical solution the shock position is of course known; the fringe shift is then computed along traces x = constant using the density and species concentrations along this line and known values of the specific refractivity for each species. This provides the theoretical data for comparison with the experimental data.

IV. GAS MODELS

The oxygen in the shock layer is assumed to be a mixture of perfect gases: molecular and atomic oxygen. The caloric equation of state includes the contribution of the low lying electronic states to the energy of the gas, which is then made up of contributions from translation, rotation, vibration and electronic excitation. The vibrational energy is computed on the basis of an anharmonic oscillator[10]. Ionization may be neglected for the present conditions.

For all the computations made the translational and rotational degrees of freedom are assumed to come into equilibrium within the shock, which is considered a surface of discontinuity. Thus,

$\tau_{tr} = \tau_{rot} = 0$ for all computations. The rotational relaxation time, though smaller than the vibrational relaxation time, is of the same order for parts of the shock layer. It is well to keep in mind that rotation and possibly translation may not have relaxed to a Boltzmann distribution when vibrational relaxation sets in.

The electronic relaxation time $\tau_{el} = 0$ for all computation, i.e. the population of the electronic levels is based on the translational temperature. There is evidence that the population of the electronic levels follows the vibrational temperature. However, as sample computations show, the effect of electronic excitation on the flow field is quite small, so that either choice should be adequate.

When the relaxation times go to the limit zero or infinity, the flow field becomes self similar. Three types of conical flows were computed, which result from the following conditions:

i) $\tau_{trans} = \tau_{rot} = \tau_{el} = 0,$

$\tau_{vib} = \tau_{diss} = \infty;$

ii) $\tau_{trans} = \tau_{rot} = \tau_{el} = \tau_{vib} = 0,$

$\tau_{diss} = \infty;$

iii) $\tau_{trans} = \tau_{rot} = \tau_{el} = \tau_{vib} = \tau_{diss} = 0.$

The first two conditions, of course, give a flow with frozen dissociation. The latter condition gives the equilibrium flow field.

Nonequilibrium flow computations are made for the case where dissociation is the only relaxation process ($\tau_{trans} = \tau_{rot} = \tau_{vib} = \tau_{el} = 0$, $0 < \tau_{diss} < \infty$), and for the case where dissociation and vibration occur simultaneously and interact with each other ($\tau_{trans} = \tau_{rot} = \tau_{el} = 0$, $0 < \tau_{vib}, \tau_{diss} < \infty$).

A model to account for the vibration-dissociation coupling was proposed in reference 5. This model accounts for the effect of vibration relaxation on the dissociation. The models of Treanor and Marrone [11, 12] and Heims [13] account additionally for the effect the dissociation has on the vibrational relaxation.

The model of Treanor and Marrone as reported in reference 12 has been used for these computations. A short outline of this model is given here. The relaxation equation for the vibrational energy E is:

$$\frac{dE}{dt} = \frac{\bar{E}\,(T_{trans}) - E}{\tau_{vib}}$$

$$- \frac{(\bar{E}\,(T_{trans}, T_{vib}) - E)}{[0_2]} \left(\frac{d[0_2]}{dt}\right)_d$$

$$+ \frac{(\bar{E}\,(T_{trans}, T_{trans}) - E)}{[0_2]} \left(\frac{d[0_2]}{dt}\right)_r$$

Here, $[0_2]$ in the notation of reference 14 is the concentration of diatomic oxygen, $(d[0_2]/dt)_d$ the rate at which molecules are dissociating; $(d[0_2]/dt)_r$ the rate at which they are recombining. $\bar{E}\,(T_{trans}, T_{vib})$ is the average vibrational energy lost in a dissociation and $\bar{E}\,(T_{trans}, T_{trans})$ is the average energy gained in a recombination. $\bar{E}\,(T_{trans}, T_{vib})$ is computed on the basis of a Boltzmann distribution as the use of a vibrational temperature implies.

For $(d[0_2]/dt)_{d,r} = 0$, the familiar equation for the relaxation of the vibrational energy of the harmonic oscillator results. The use of this equation in the case of an anharmonic oscillator as is done here, and in reference 12, is not strictly correct.

The effect of vibrational relaxation on dissociation is included through the vibrational coupling factor V

$$V \equiv k_d/k_{deq}$$

where k_d is the actual dissociation rate constant; k_{deq} the dissociation rate constant that would exist with vibrational equilibrium at the local translational temperature.

Postulating a probability of the form

$$P_i = \frac{1}{Q(T_F)} \exp\ (E_i/kT_F)$$

for dissociation from the ith vibration level, V is found as:

$$V = \frac{Q\ (T_{trans})\ Q\ (T_F)}{Q\ (T_{vib})\ Q\ (-U)}$$

here

$$\frac{1}{T_F} = \frac{1}{T_{vib}} - \frac{1}{T_{trans}} - \frac{1}{U}$$

U is an adjustable constant taken to be U = D/6k in the numerical computation reported here. D is the dissociation energy, Q the vibrational partition function and k the Boltzmann constant.

The criticism raised against this model[14] concerns the fact that the dissociation probability is postulated and the assumption of a Boltzmann distribution in the vibrational mode is made.

A consistent treatment of the coupled vibration-dissociation process for the dissociation of diatomic molecules in an inert background gas has been given by Keck and Carrier[15].

In reference 12 Marrone and Treanor have applied their model to this case: dissociation of O_2 in an argon bath. For this case then, the findings of reference 15 may be listed here for the purpose of evaluating Treanor and Marrone's phenomenological model: the coupled vibration-dissociation occurs in two steps; in the first phase the vibrational mode relaxes to a population distribution which is not a Boltzmann but rather an "almost" Boltzmann distribution. During this phase dissociation is negligable. In the second phase which is much longer dissociation proceeds without changing the "almost" Boltzmann distribution.

The theory of the second phase is treated classically and quantum-mechanically in reference 15. The main result is that the usual phenomenological rate equation is valid; however, the rate constants are depressed below their equilibrium value (see references 14 and 16).

In reference 15a, the fast process is treated for the case of a harmonic oscillator and it is shown that this phase gives rise to incubation times. These have been experimentally observed. These incubation times were predicted by Marrone and Treanor as well as the reduced rate constant k_d during the quasi-steady second phase. Indeed, the comparison made in reference 12 shows good agreement with experimental incubation times[17] and the rate constant k_d.

On the basis of this comparison, one can expect Treanor and Marrone's model to give at least qualitatively correct results. For the present purpose, it is important that this model can be applied formally to the dissociation in pure oxygen, and further that it is still simple enough to be used in flow field computation.

V. RATE COEFFICIENTS AND VIBRATIONAL RELAXATION TIMES

A. Constant Efficiency Model

The interpretation of the rate constants measured in shock tubes is made difficult because most of the rates are measured under conditions where coupling is important. The so-called pre-exponential factor shows an inverse temperature dependence, which can be caused by non-equilibrium effects in the dissociating molecule[14,15,18]. Such a pre-exponential factor has been found in the experiments by Camac and Vaughan[19] for the dissociation of O_2 in an argon bath. Indeed, their rate coefficient is of the form given by reference 14.

In order not to account twice for the coupling the pre-exponential factor should be removed from the rate expression. This has not been done, as will be seen below, there exists an even stronger temperature dependence on the pre-exponential factor for the case of dissociation in pure oxygen for which there is currently no explanation.

All the computations done are based on Camac and Vaughan rate constants. In order to apply their results to the dissociation of pure oxygen the relative efficiency of O_2 and O with respect to A has to be

known. If the rate coefficient is written in the form

$$k_d\ (O_2 - O, O_2) = Z_o\ (O_2 - O_2, O) \cdot$$

$$P^*\ P(O_2 - A)\ e^{-D/RT}$$

where $P\ (O_2 - A)$ is defined by the equation

$$k_d\ (O_2 - A) = Z_o\ (O_2 - A)\ P\ (O_2 - A)\ e^{-D/RT};$$

then we may consider P* the efficiency of O_2 and O relative to argon. Z_o is the bimolecular collision rate for unit concentrations of the reactants. Wray[20] has made a recommendation which amounts to taking this efficiency to be a constant independent of temperature, at least for the low temperature regime.

This recommendation has been widely followed in nonequilibrium computations even in the high temperature regime. Such a constant factor can be explained on the basis of transfer of rotational energy of the colliding molecule into vibrational energy of the dissociating molecule (reference 14). The computations made with this assumption of constant relative efficiency are labeled "P* = constant" in this report. The vibrational relaxation time for the $(O_2 - O_2)$ collisions in these computations was taken from Camac[21] and extrapolated to the temperatures encountered in these experiments according to the Landau-Teller formula.

B. Variable Coefficients

Measurements of the rate coefficients of pure oxygen show that the relative efficiency P* is a function of T. For $O_2 - O_2$ collisions this is demonstrated in reference 14. For use in the present computation the relative efficiency P* is assumed of the form $P^*\ (O_2 - O_2) \sim C\ (D/RT)^n$. The constants C and n are determined such that Wray's recommended value of P* is reached for T = 4,000°K, and for T = 7,000°K a value of P* is reached that is suggested on the basis of Camac and

Vaughan's measurements. P* as a function of T is plotted in Figure 4. Also plotted are values of P* based on the rate constants measured by Generalov (3,000 - 7,000°) and Matthews (3,000 - 5,000°).

Atomic oxygen has been found highly effective in O_2 - O collisions at low temperatures; however, at high temperatures Wray[17] noticed a drastic decrease in atomic oxygen efficiency, the efficiency approaching that of argon at very high temperatures. Again, assuming $P^* \sim C\,(D/RT)^n$, C and n are determined from the value of P* at 6,000°K (Camac and Vaughan)[19] and the value of P* at 17,000°K according to reference 17. The resulting dependence of P* on T is shown in Figure 4.

In the vibrational excitation process a similar decrease in efficiency of oxygen molecules relative to argon has been observed by Generalov as reported in reference 14. Oxygen molecules are about five times more effective than argon in exciting molecular vibration in the low temperature regime (< 5,000°K). At high temperature the efficiency of oxygen decreases and becomes equal to the argon efficiency. The vibrational relaxation time in the computations for variable efficiency were taken accordingly to be the relaxation times for (O_2 - A) collisions, since the major adjustments in vibrational energy occur in the high temperature part of the shock layer. See Figure 5 for theoretical temperature distribution in the shock layer. It may be mentioned that (according to reference 14) extrapolating the relaxation time for pure oxygen according to the Landau-Teller formula leads to relaxation times which are smaller than actual times.

The computations made for variable efficiency and the increased vibrational relaxation times are labeled P* = f(T) in the figures.

It is seen that for both cases of variable and constant efficiency the reaction rates and relaxation times had to be extrapolated and interpolated to a region where no data are available at this time. Most disturbing is the fact that no satisfactory explanation for the strong temperature dependence of the relative efficiencies exists. As will be seen, this has a large effect on the predicted flow field. This, of

course, makes the matter of extrapolating the rate constants and relaxation times a questionable practice.

VI. COMPARISON OF NUMERICAL AND EXPERIMENTAL DATA

Case 1 will be discussed first. Figure 6 shows the shock position and Figure 7 the shock layer "thickness."

The experimental points plotted are points obtained from several independent measurements of the same interferogram. The shock location in an interferogram is not as clearly defined as for example in a schlieren picture and the different measurements lead to a scatter, which on the scale of Figure 7 is quite pronounced. It is seen that the equilibrium flow assumption ($\tau_{vib} = \tau_{diss} = 0$) and the nonequilibrium flow assumption with ($\tau_{vib} = 0$, $0 < \tau_{diss} < \infty$) yield practically the same shock layer thickness and can hardly be distinguished even on the scale of Figure 7.

Predictions based on these two models give shock layer thickness 30-40% smaller than experiment. The shock layer thickness for the coupled vibration-dissociation model and $P^* = \text{const}$ gives better agreement with experiment but the thickness is still seen to be about 20-30% too small. Best agreement is reached for the coupled model and $P^* = f(T)$. Shown also in Figure 7 are the two conical flows resulting from $\tau_{vib} = \tau_{diss} = \infty$ and $\tau_{vib} = 0$, $\tau_{diss} = \infty$. The latter model yields a shock shape which is in as good or better agreement than the equilibrium flow shock shape. Superficial estimate of the flow for the free stream conditions given would suggest an equilibrium flow.

Figure 8 shows the fringe shift δ in units of undisturbed fringe spacing for the various models in comparison with experimental data, for one trace at $x = 14.72$ mm. The fringe shift in the shock layer is plotted as a function of the distance r from the axis to the point for which δ is measured. The fringe shift is computed using experimental refractivities of reference 21. These are in good agreement with earlier measurements of Alpher and White[22].

In the computation the refractivities have been assumed independent of the temperature in the temperature range of the shock layer. In the temperature range of 3,000-4,500°K this has been shown to be the case for the oxygen atom and molecule by Anderson[21]. There is no experimental data available for the refractivities at higher temperatures. The ratio of specific refractivity at 4,000°K to the specific refractivity at 12,000°K of the oxygen atom was found to be 1.00 on the basis of Kramer's dispersion formula and using the best f-numbers available. The absolute value thus computed is, however, not in agreement with experimental data.

The refractivities of high temperature gases are not reliably known at this time, and this introduces an additional uncertainty in this data. However, the conclusions concerning the shock layer thickness are not affected by the value of specific refractivity; further, the fringe shift computed on the basis of constant refractivity is consistent with the shock data as inspection of Figures 8 and 9 shows.

In computing the fringe shift the value of the free stream density ρ_∞ is used. Within the experimental error of ρ_∞ the density used in the computation is selected to give at <u>one</u> point on the body, the same fringe shift as the experimental fringe shift at this point. This required a change of free stream density by 10% from the value initially determined from the streak interferogram. Two sets of data points plotted in Figures 8 and 9 result from two independent measurements from the same interferogram. The scatter is indicative of the accuracy of measuring the fringe shift. The traces closer to the tip (x = 10.31; x = 11.78 mm) show the largest scatter. The uncertainty in shock position on the upper side of Figure 1 where the trace was taken is approximately indicated by the error bars. The graph shows that best agreement with the experimental data is reached for the coupled vibration-dissociation model with $P^* = f(T)$. Figure 9 gives the fringe shift for various traces. The only theoretical curve in this figure is the curve based on the coupled model with variable efficiency.

For certain conditions, namely if $\Sigma K_i \rho_i$ is constant in the shock layer (K_i is the specific refractivity and ρ_i the partial density) the fringe shift data can be used to obtain the density distribution. Assuming constant refractivities, the above condition is fulfilled in this case. The density distribution for various traces are shown in Figure 10.

The traces near the tip have not been used, since they have a higher experimental error. The computation based on the coupled model with variable efficiency $P^* = f(T)$ give best agreement with experiment. The equilibrium flow computation yields density values about 30% too high. The computation for the uncoupled model ($\tau_{vib} = 0$, $0 < \tau_{diss} < \infty$) was not carried far enough in x to serve for comparison here; however, the traces closer to the tip show that the density distribution very closely duplicates the distribution of the equilibrium flow except for a very steep rise near the shock. The numerical computations for this model were very time consuming because a small grid size had to be used to handle the strong gradients in the flow variables near the shock.

The coupled vibration-dissociation model with constant efficiency $P^* = \text{const}$ gives density-distribution about 20% too high.

The experiment for case 2 was done in a modified expansion tube[23]. In this modification the test gas is processed by a reflected shock which heats the test gas high enough to dissociate it. The test gas is subsequently expanded from this dissociated state and nonequilibrium in the free stream may be expected. For the conditions of this experiment the compressibility in the reflected region depends very sensitively on the Mach number of the reflected shock, so that the compressibility in the free stream is uncertain even if no recombination occurs in the expansion process. The nominal value of the free stream compressibility based on the Mach number of the reflected shock and assuming a completely frozen expansion process in $Z_\infty = 1.1$, giving an atom concentration of $C_0 = 0.23$ and a molecule concentration of $C_{O_2} = 0.855$, here $C_i = (\rho_i/\rho)/(W_i/W_{O_2})$ and W is the molecular weight. In addition, the

vibrational energy is assumed frozen out in the expansion and the free stream vibrational energy is based on the (equilibrium) temperature in the shock reflected region.

In the computation of this flow an attempt has been made to correct for the boundary layer thickness effect. Some of the computation for this case is made for a body which is made up of the cone plus the displacement thickness. The displacement thickness is computed on the basis of an ideal gas of constant γ. For the highly cooled boundary layer the thickness is proportional to the square of the surface Mach number, and is about twice as large in case 2 as in case 1.

Since the resulting body would have a blunted tip a conical forebody has been attached to the tip, which has the largest possible angle consistent with an attached shock and purely supersonic flow for the given free stream Mach number. The conical tip with half angle of 38.5° attaches to the body where the slopes of their generating curves are the same. The combined body is 0.001mm longer than the original cone. The computed density profiles for this body are found to be essentially the same as for the cone, except displaced radially by the displacement thickness.

Figure 11 shows the shock position and Figure 12 the shock layer thickness.

The computations are carried only to 20mm because at this point the memory capacity of the computing machine was exceeded.

In this case, the effect of vibration-dissociation coupling on the shock layer flow should be reduced, since the maximum temperature in the shock layer is only 8,600°K. However, as Figure 12 shows, the effect of boundary layer becomes noticeable and the free stream dissociation has a large effect on the flow field. The value of Z_∞ is not well known in this experiment and this should be considered when comparing the experiments and theory plotted in Figure 12. However, it is seen that the model with variable efficiency gives the best agreement with experiment. Just as in case 1, even this model predicts a shock layer somewhat too small.

VII. CONCLUSIONS

Experiments of nonequilibrium flows around cones in oxygen have been compared with numerical prediction. The free stream conditions are such that the flow field in the shock layer is determined by various overlapping relaxation processes. Of these, only the coupling between vibration and dissociation relaxation processes has been considered, although an effect of rotational and possibly translational non-equilibrium must be expected for portions of the shock layers.

The coupling between vibration and dissociation has been treated with a phenomenological model which is simple enough to be used in flow field computations and still retains the main features of the chemical kinetic process. Best agreement with experiments was obtained for the model that accounted for variable effectiveness of O_2 and O collisions in the excitation of vibration and dissociation. There is experimental evidence for decreased efficiency at high temperature, but since there is no satisfactory theoretical explanation, the extrapolations in the rate coefficients and relaxation times used in these computations must be considered with caution.

It is shown here, that the usual practice of neglecting coupling effects leads to an inaccurate description of the flow field. Conditions where coupling becomes important are encountered for situations of practical interest. In this connection it may be mentioned that based on binary scaling the flow fields considered here are representative for flight of a body say of 1 foot diameter at 140,000 ft. altitude in an oxygen atmosphere at 20,000 ft/sec velocity. In air the analysis of the flow field under similar conditions is rendered much more difficult because many coupled relaxations occur that are presently not sufficiently understood.

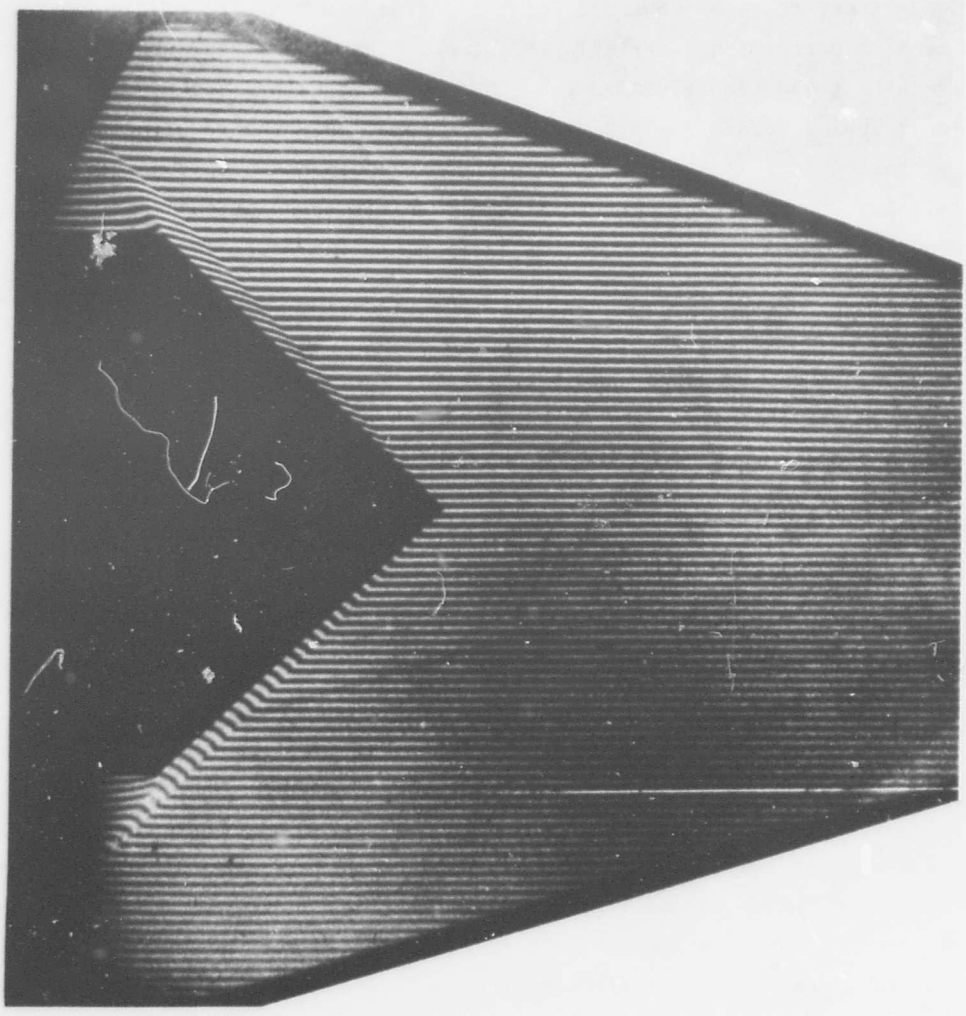

Figure 1. Frame interferogram of a hypersonic flow around a cone. Case 1, observing wavelength: λ = 4358Å, free stream conditions: U_∞ = 6350 m/sec, ρ_∞ = 0.0148 kg/m^3, p_∞ = 4810 N/m^2.

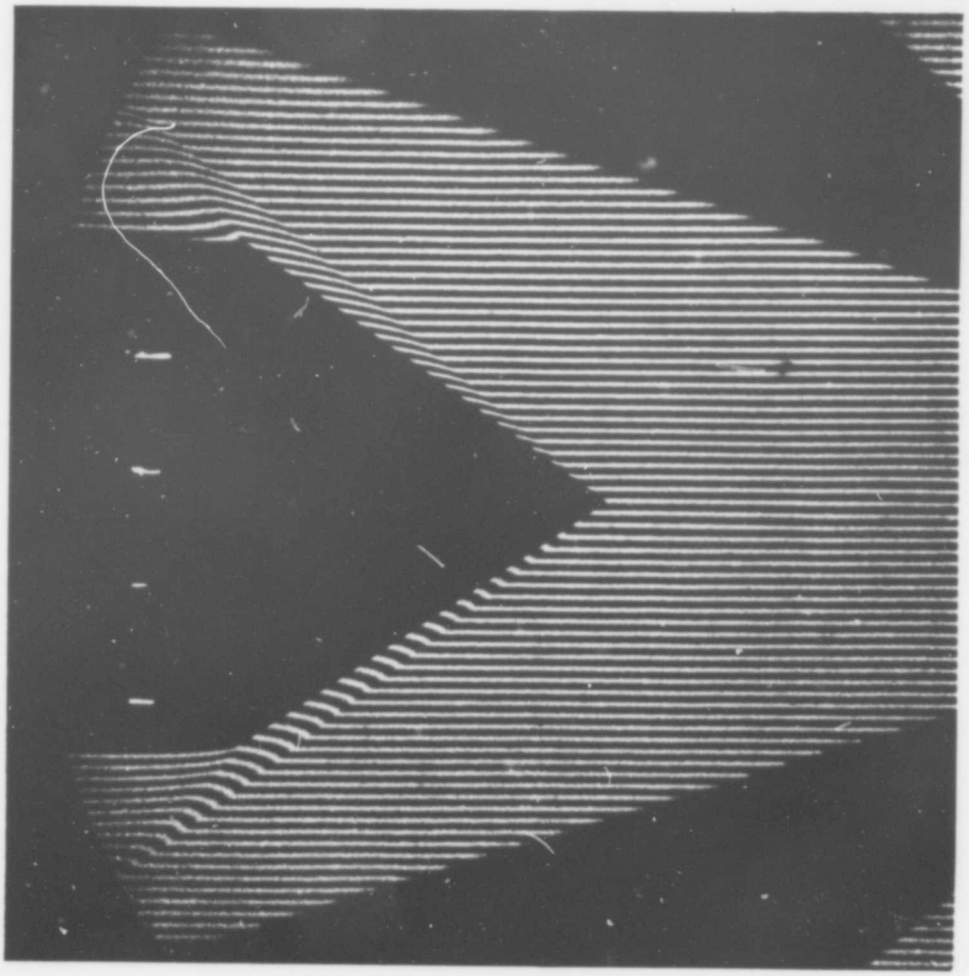

Figure 2. Frame interferogram of a hypersonic flow around a cone. Case 2, observing wavelength: λ = 5461 Å, free stream conditions: U_∞ = 5710 m/sec, ρ_∞ = 0.0194 kg/m^3, p_∞ = 5720 N/m^2.

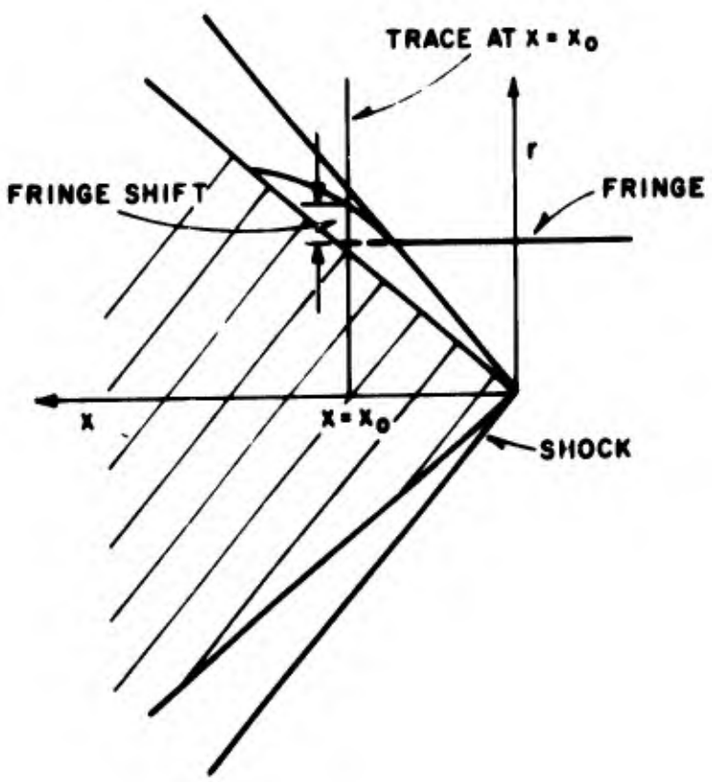

Figure 3. Sketch illustrating the coordinate system

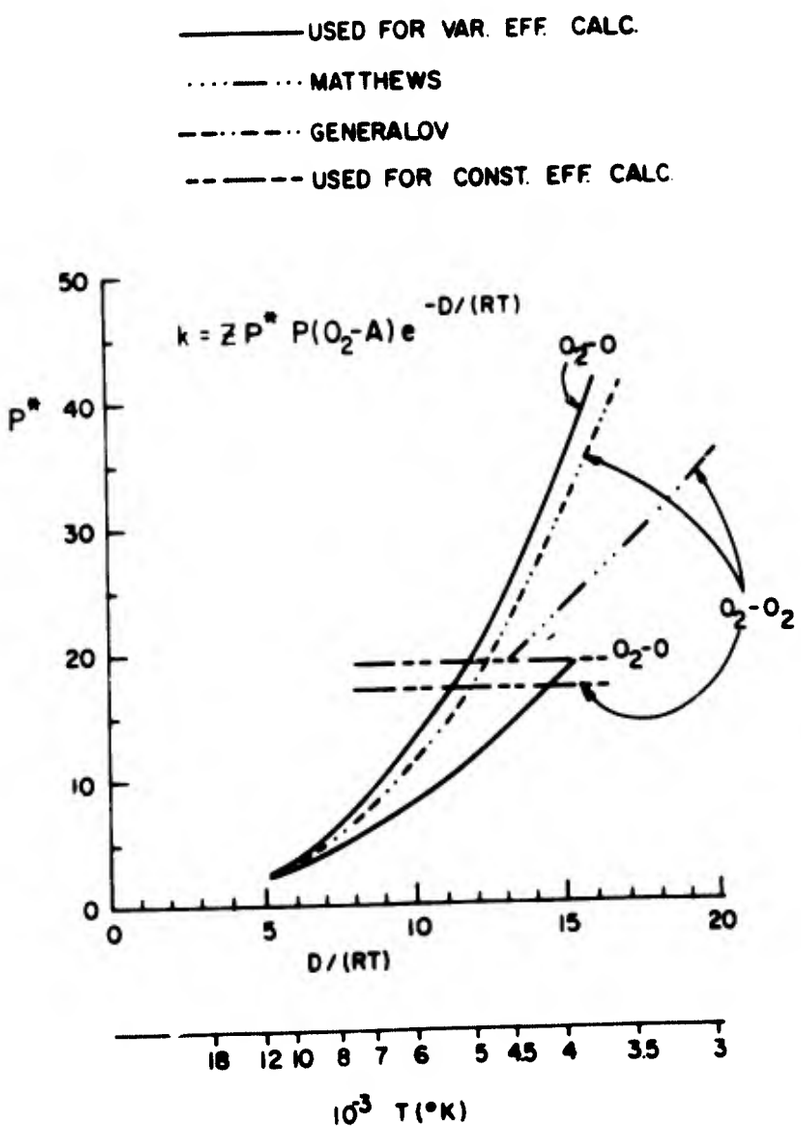

Figure 4. Relative efficiency P* as f(T)

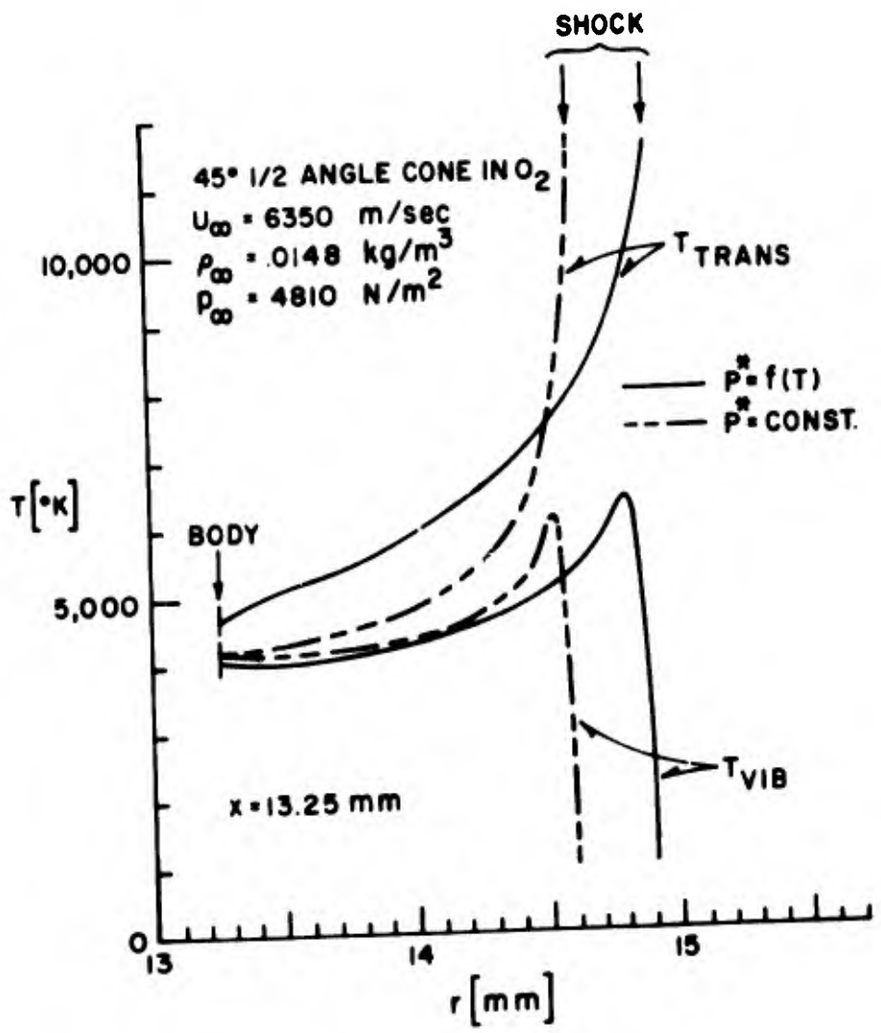

Figure 5. Theoretical temperature distribution in the shock layer. Case 1.

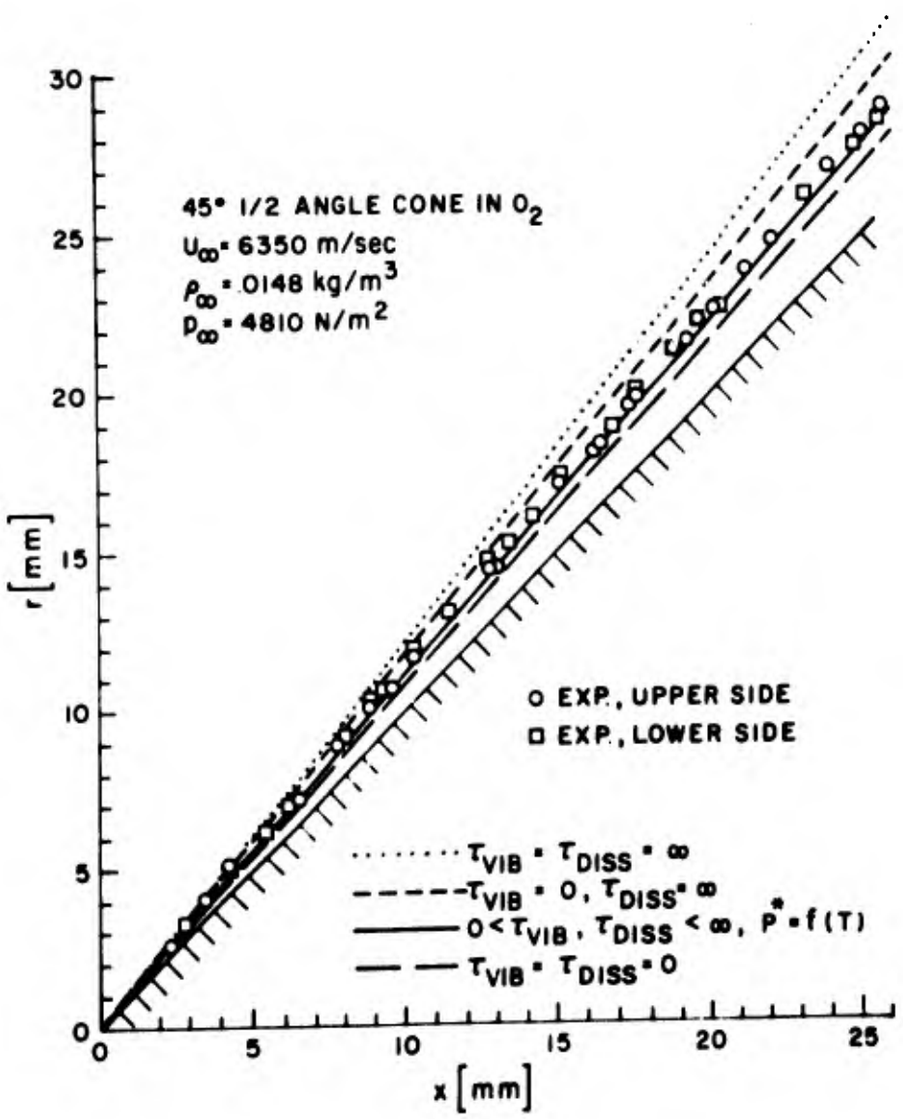

Figure 6. Comparison of the experimental and theoretical shock position. Case 1.

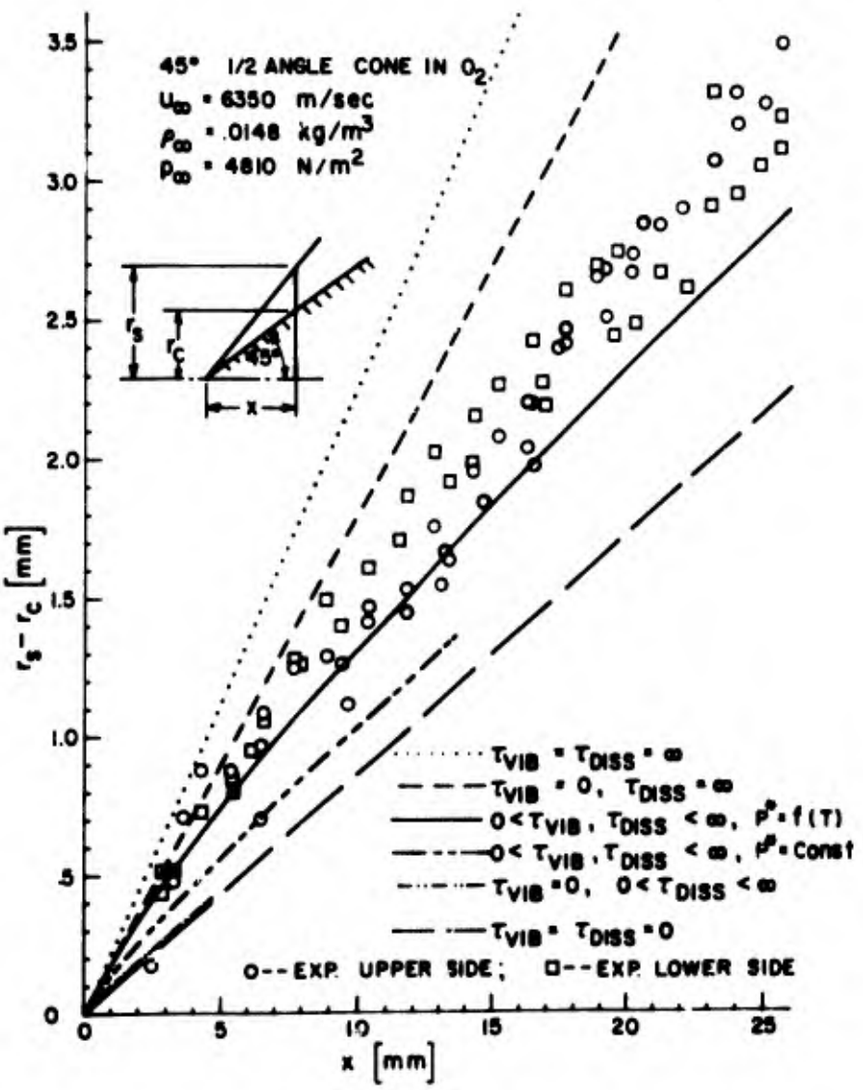

Figure 7. Comparison of the experimental and theoretical shock layer "thickness". Case 1.

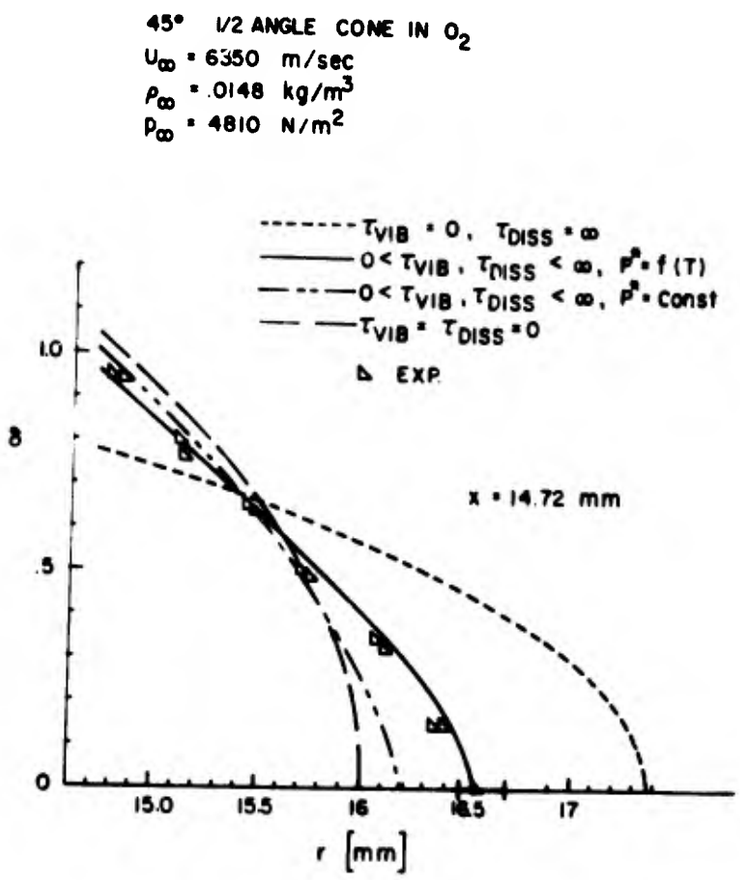

Figure 8. Comparison of experimental and theoretical fringe shift $\delta(r)$

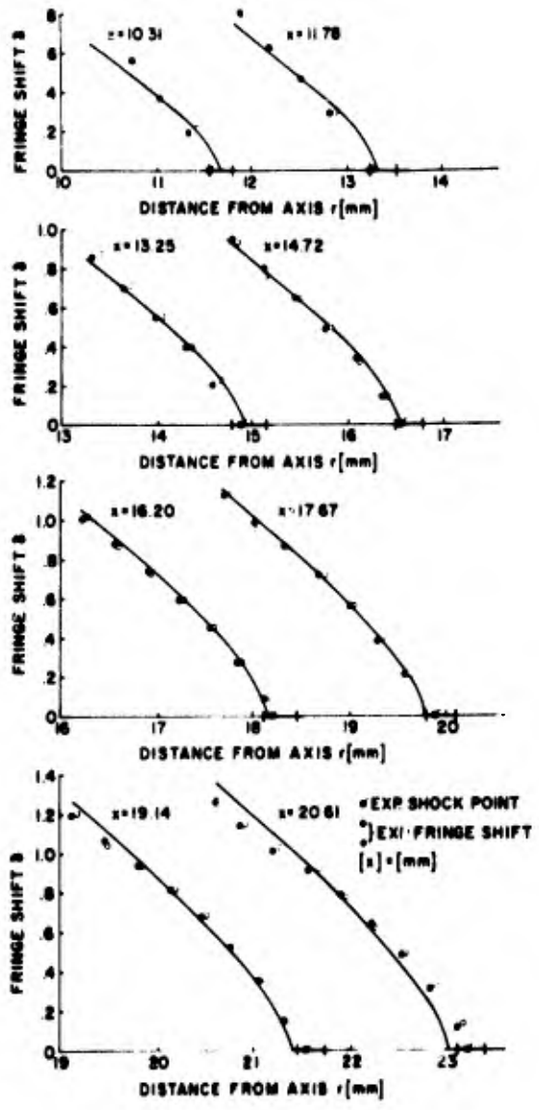

Figure 9. Comparison of experimental fringe shift $\delta(r)$ with theoretical prediction using $0 < \tau_{vib}, \tau_{diss} < \infty$ and $P^* = f(T)$

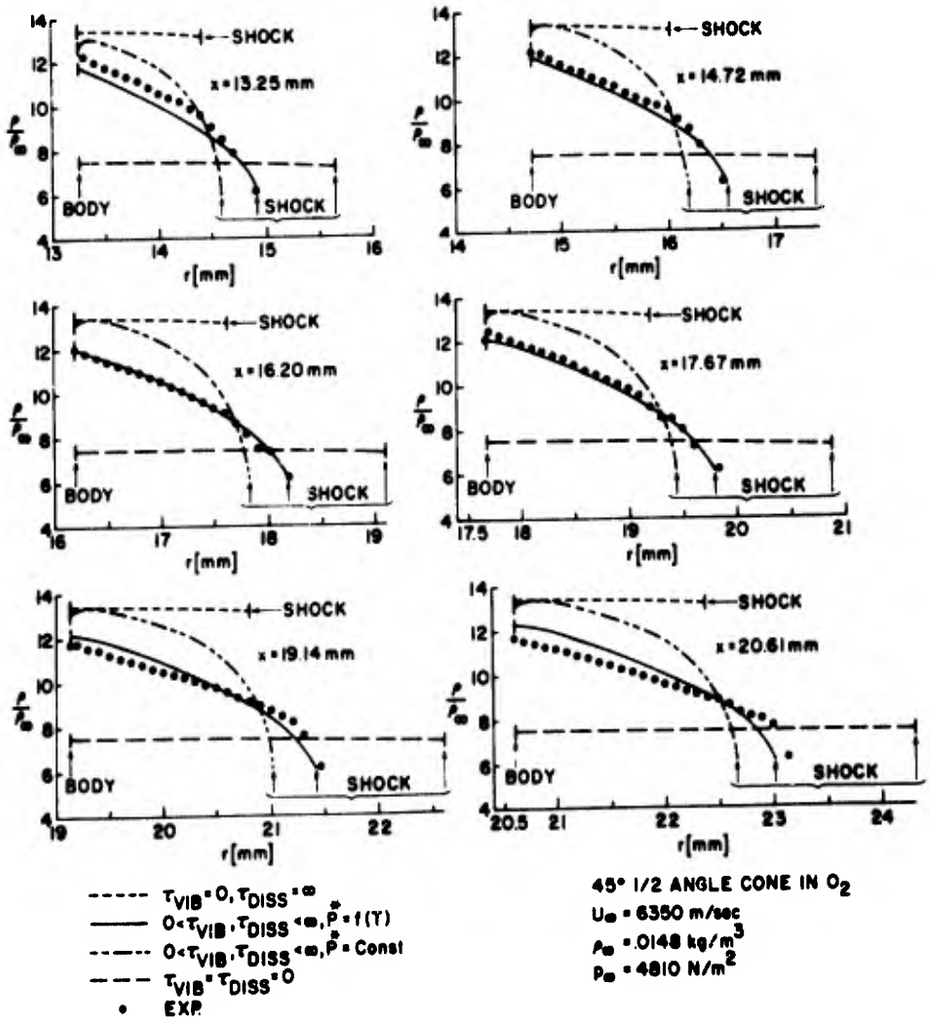

Figure 10. Comparison of the experimental density traces with theoretical predictions

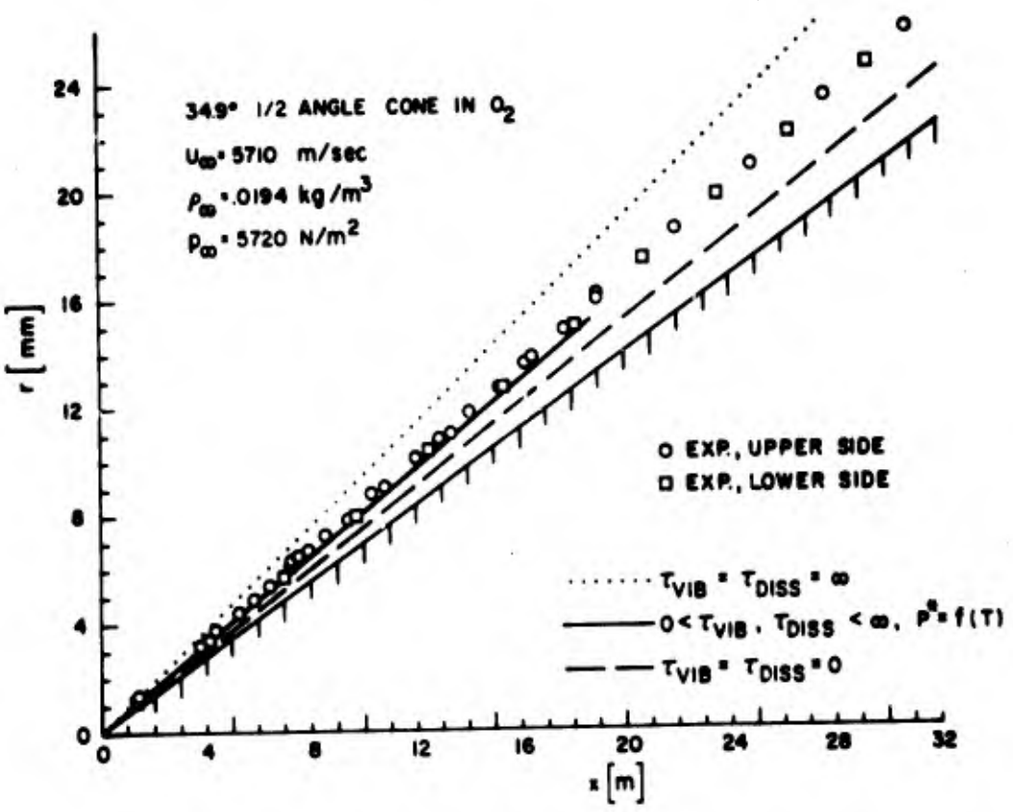

Figure 11. Comparison of the theoretical and experimental shock shape. Case 2.

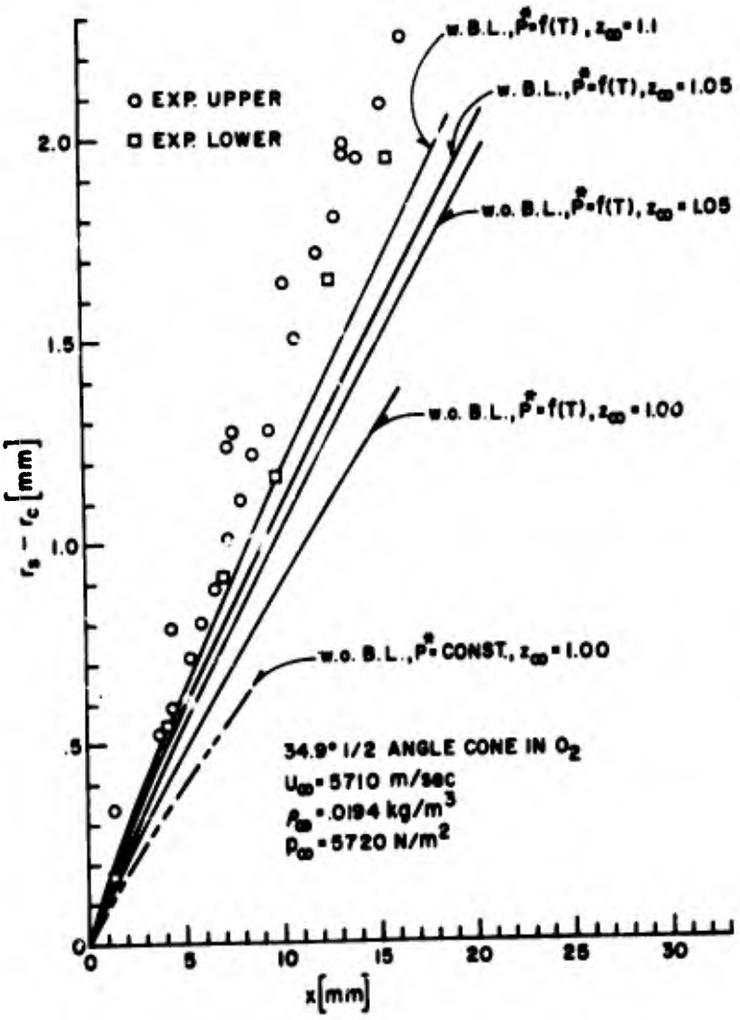

Figure 12. Comparison of the theoretical and experimental shock layer thickness. Case 2.

REFERENCES

1. J. G. Hall, A. Q. Eschenroeder, and P. V. Marrone, J. Aero. Sci. 29, 1962, pp. 1038-1051.

2. A. D. Wood, J. F. Springfield, and A. J. Pallone, AIAA J. 2, 1964, pp. 1697-1705.

3. J. H. Spurk, N. Gerber, and R. Sedney, AIAA J. 4, 1966, pp. 30-37.

4. J. H. Spurk and J. M. Bartos, Phys. Fluids 9, 1966, pp. 1278-1285.

5. P. Hammerling, J. D. Teare, and B. Kivel, Phys. Fluids 2, 1959, pp. 422-426.

6. S. C. Lin and W. I. Fyfe, Phys. Fluids 6, 1963, pp. 1215-1221.

7. J. H. Spurk, Proceedings of the Fourth Hypervelocity Techniques Symposium, 1965, pp. 111-145.

8. J. H. Spurk, D. T. Knauss, and J. M. Bartos, AGARD Conference Proceedings No. 12, 1967, pp. 569-593.

9. J. H. Spurk and E. J. Gl[illegible]n, AIAA to be published.

10. G. Hertzberg, Spectra of Diatomic Molecules, D. Van Nostrand Company, Inc., New York, 2nd edition.

11. C. E. Treanor and P. V. Marrone, Phys. Fluids 5, 1962, pp. 1022.

12. P. V. Marrone and C. E. Treanor, Phys. Fluids 6, 1963, pp. 1215-1221.

13. S. P. Heims, J. Chem. Phys. 38, 1963, pp. 603.

14. Ye. V. Stupochenko, S. A. Losev, and A. I. Osipov, Relaxation in Shock Waves, Springer-Verlag, New York, 1967.

15. J. Keck and G. Carrier, AVCO Research Report 212, 1965.

15a. C. A. Braun, J. C. Keck, and G. F. Carrier, AVCO Research Report 243, 1966.

16. A. I. Osipov and E. V. Stupochenko, Soviet Physics Uspekhi 6, 1963, pp. 43-66.

17. K. L. Wray, J. Chem. Phys. 37, 1962, pp. 1254-1262.

18. B. Widom, J. Chem. Phys. 34, 1961, pp. 2050-2056.

19. M. Camac and A. Vaughan, J. Chem. Phys. 34, 1961, pp. 460-470.

20. K. L. Wray, Hypersonic Flow Research, F. R. Ridell Ed., Academic Press, Inc., New York, 1962.

21. J. H. B. Anderson, UTIAS Tech. Note No. 105, 1967. See also J. H. B. Anderson, et. al, Phys. Fluids, 1967, pp. 1848.

22. R. A. Alpher and D. R. White, Phys. Fluids 2, 1959, pp. 153-161.

23. J. H. Spurk, E. J. Gion, and W. B. Sturek, AIAA Paper No. 68-311.

UNCLASSIFIED

Security Classification

DOCUMENT CONTROL DATA - R & D

(Security classification of title, body of abstract and indexing annotation must be entered when the overall report is classified)

1. ORIGINATING ACTIVITY (Corporate author) U.S. Army Aberdeen Research and Development Center Ballistic Research Laboratories Aberdeen Proving Ground, Maryland	2a. REPORT SECURITY CLASSIFICATION Unclassified 2b. GROUP

3. REPORT TITLE

EXPERIMENTAL AND NUMERICAL NONEQUILIBRIUM FLOW STUDIES

4. DESCRIPTIVE NOTES (Type of report and inclusive dates)

5. AUTHOR(S) (First name, middle initial, last name)

Joseph H. Spurk

6. REPORT DATE May 1969	7a. TOTAL NO. OF PAGES 42	7b. NO. OF REFS 23
8a. CONTRACT OR GRANT NO. b. PROJECT NO. RDT&E 1T061102A33D c. d.	9a. ORIGINATOR'S REPORT NUMBER(S) Report No. 1445 9b. OTHER REPORT NO(S) (Any other numbers that may be assigned this report)	

10. DISTRIBUTION STATEMENT

This document has been approved for public release and sale; its distribution is unlimited.

11. SUPPLEMENTARY NOTES	12. SPONSORING MILITARY ACTIVITY U.S. Army Materiel Command Washington, D.C.

13. ABSTRACT

Experimental and numerical studies of the nonequilibrium shock layer around cones in hypersonic pure oxygen flows are reported. Experimental conditions are such that rotational, vibrational and dissociation relaxation occur simultaneously. Attention is given to the effect of coupled relaxation on the flow properties in the shock layer. The phenomenological models of Hammerling, et al, and Treanor and Marrone predict the flow field qualitatively correct. However, quantitative differences in shock geometry and density distribution are appreciable. Better quantitative agreement with experiment is reached if in these models a temperature dependent efficiency of O_2 and O in the relaxation processes is assumed.

DD FORM 1 NOV 68 1473 REPLACES DD FORM 1473, 1 JAN 64, WHICH IS OBSOLETE FOR ARMY USE.

UNCLASSIFIED

Security Classification

14. KEY WORDS	LINK A		LINK B		LINK C	
	ROLE	WT	ROLE	WT	ROLE	WT
Nonequilibrium Flow						
Dissociation						
Oxygen						
Vibrational Relaxation						
Hypersonic Flow						
Coupled Vibration and Dissociation						
Rate Constants						
High Energy Flow - Cones						